Journal of Power Sources 226 (2013) 94–100

Contents lists available at SciVerse ScienceDirect

Journal of Power Sources

journal homepage: www.elsevier.com/locate/jpowsour

Verification of necessity of one-dimensional titania nanoscale materials for dye-sensitized solar cells

Motonari Adachi [a,*], Ryo Tanino [b], Jun Adachi [c], Yasushige Mori [b], Katsumi Tsuchiya [b], Seiji Isoda [d], Fumio Uchida [a]

[a] Fuji Chemical Co., Ltd., 1-35-1 Deyashikinishi-machi, Hirakata 573-0003, Japan
[b] Department of Chemical Engineering and Materials Science, Doshisha University, 1-3 Miyakodani, Tatara, Kyotanabe 610-0321, Japan
[c] National Institute of Biomedical Innovation, 7-6-8 Asagi Saito, Ibaraki 567-0085, Japan
[d] Institute for Integrated Cell-Material Sciences (iCeMS), Kyoto University, Yoshida-Ushinomiya, 606-8501 Kyoto, Japan

HIGHLIGHTS

- Three one-dimensional titania nanoscale materials synthesized in our laboratory show high conversion efficiency around 9%.
- Necessity of highly crystallized 1-dimensional titania nanoscale materials was elucidated by theoretical consideration.
- The consideration was verified by systematic experiments based on the measurements of (I–V) relation and EIS analysis.

GRAPHICAL ABSTRACT

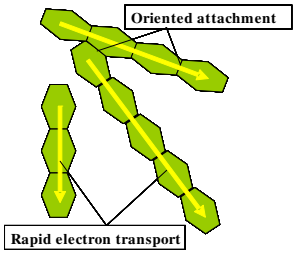

Necessity of highly crystalline 1-dimensional titania nanoscale materials was elucidated by theoretical consideration and verified by experiments.

ARTICLE INFO

Article history:
Received 25 September 2012
Accepted 12 October 2012
Available online 30 October 2012

Keywords:
One-dimensional
Titania
Nanoscale materials
Dye-sensitized solar cell
Impedance spectroscopy

ABSTRACT

Necessity of highly crystallized 1-dimensional titania nanoscale materials (1DTNM) was elucidated by theoretical consideration based on both the electron transfer processes shown by Nyquist plots obtained in electrochemical impedance spectroscopy (EIS) and current–voltage (I–V) measurements. The consideration was verified by systematic experiments, in which titania nanowires (TNWs) with network structure were chosen as a highly crystallized 1DTNM. The cells with electrodes made of various TNW content from 0% to 100% of TNWs mixed with P-25 were fabricated. Based on the measurements of I–V relationship and EIS measurements of these cells, the following three points were clearly demonstrated as verification of the consideration; 1) resistance of electron transport in the titania electrode to the conducting glass electrode is small, 2) the ratio of the resistance for the recombination reactions against that for the transport rate to the conducting glass electrode is large, i.e., efficiency of electron collection is high, and 3) electron density in the titania electrode is high. These points are essentially important to realize high efficiency in DSSCs.

1. Introduction

Light from the sun is the ideal source of energy. Fortunately, the supply of energy is gigantic, i.e., 3×10^{24} J year^{-1} or about 10^4 times more than what mankind consumes currently. The energy demand is expected to touch 30 TW by 2050 [1,2]. Dye-sensitized solar cells (DSSCs) have attracted much attention as they offer a possibility of extremely inexpensive and efficient solar energy conversion. In 1991, O'Regan and Grätzel [3] published a remarkable report, and the Grätzel group attained 10% efficiency in 1993 [4]. The system already reached conversion efficiency 12.3% [5], which exceeds the level to supply electricity at the rate of home use, i.e., 10%. Nevertheless, the

* Corresponding author. Tel.: +81 72 849 6551; fax: +81 72 848 1367.
E-mail address: mo-adachi@fuji-chemical.jp (M. Adachi).

0378-7753/$ – see front matter © 2012 Elsevier B.V. All rights reserved.
http://dx.doi.org/10.1016/j.jpowsour.2012.10.024

energy conversion efficiency of the cells for commercial devices has not yet reached the level, which provides lower cost than that of conventional methods of electricity generation using fossil fuel. Therefore, attainment of higher efficient cells is one of the most important challenges for the dye-sensitized solar cells.

Titanium dioxide is the most promising material for the electrode of DSSCs. Many investigators have improved the anodic electrode over 10 years [6–14]. Since 1991, various improvements to the TiO_2 electrode in the DSSCs have been made in terms of light absorption, light scattering, charge transport, suppression of charge recombination, and improvement of the interfacial energetics. In order to prevent contact between the redox mediator in the electrolyte and the fluorine doped tin oxide (FTO), a TiO_2 blocking layer (around 50 nm thick) prepared by chemical bath deposition, spray pyrolysis, or sputtering is used [6]. A light scattering layer on the top of the mesoporous film, consisting of an around 3 μm porous layer containing around 400 nm sized TiO_2 particles [7,8]. Voids of similar size in a mesoporous film can also give effective scattering [9]. The $TiCl_4$ treatment leads to the deposition of an ultrapure TiO_2 shell (around 1 nm) on the mesoporous TiO_2 [10], resulting in increased dye adsorption due to increased roughness [6,11,12]. For flexible polymer cells, a compression technique was developed [13,14].

One-dimensional titania nanoscale materials (1DTNM) have been investigated for attainment of highly efficient solar cells [15–25]. One of the earliest papers describing the utility of one-dimensional TiO_2 nanoscale materials in DSSCs was ours describing application of single crystalline TiO_2 nanotubes for DSSCs [2,15]. This early research has spurred further activity of one-dimensional nanostructured in DSSCs. Ohsaki et al. [16] improved the Kasuga's method of synthesis of titania nanotubes (TNTs) [17,18] by high temperature sintering (higher than 700° C) and fabricated anatase TNTs, attaining 7.1% conversion efficiency. Higher efficiency 8.9% was obtained for the same system by Hsaio et al. [19] Kim et al. [20] used electrophoretic deposition of TNTs and attained 6.7% efficiency. Wei et al. [21] fabricated large surface area 117 m^2/g using TNTs and got 7.5% conversion efficiency. By replacing nanoparticulate films with one-dimensional materials, charges are allowed to move only in one-dimension instead of randomly in three-dimension. The directed movement improves cell currents and reduces losses by increasing the residence lifetime of charge carriers, typically measured with intensity modulated photovoltage spectroscopy (IMVS) for titania nanotube arrays [22]. Many one-dimensional architectures were developed, such as titania nanotube arrays by anodic oxidation [22–28], carbon nanotube–TiO_2 composite nanostructures [29–33], and electrospun anisotropic TiO_2 [32–35]. High conversion efficiencies 9.1% [28], 10.6% [32], and 9.52% [34] were obtained for the above investigations of titania nanotube arrays, carbon nanotube–TiO_2 composite, and electrospun method, respectively.

It is important to make clear the reason for necessity of 1DTNM for attainment of higher efficient DSSCs through theoretical consideration and its verification based on the experimental evidences. In this article first we present that DSSCs with electrodes composed of three kinds of highly crystalline 1DTNM synthesized in our laboratory, i.e., single crystal-like network structure of titania nanowires (TNWs) [36], titania nanorods (TNRs) [37] and newly synthesized titania nanochains (TNCs, Fig. 1), showed high light-to-electricity conversion efficiency around 9%. Next, necessity of highly crystalline 1DTNM for fabricating highly efficient DSSCs is deduced based on the theoretical consideration of electron transport processes derived from Nyquist plots obtained by electrochemical impedance spectroscopy (EIS) and *I–V* measurement. We verify then the consideration by an intentional experiment, measuring the electron transport properties by EIS on the cells with

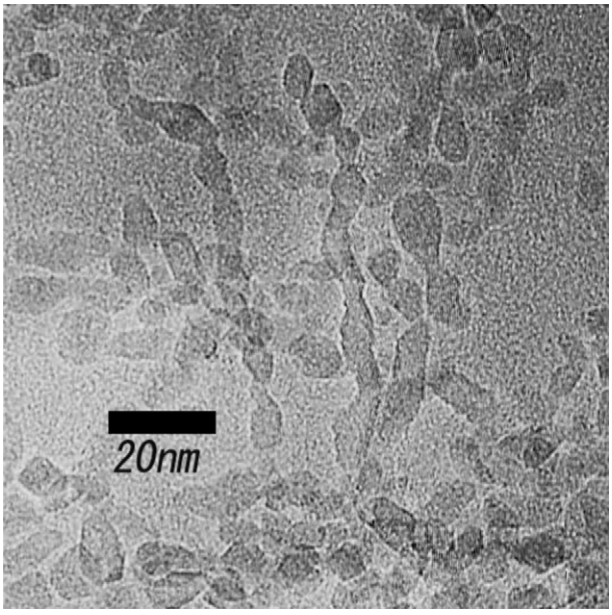

Fig. 1. TEM image of titania nanochains.

electrodes made of single crystal-like TNWs, a representative of highly crystalline 1DTNM, and P-25 with various TNW contents.

2. Experimental

2.1. Formation of single crystal-like network structure of titania nanowires (TNWs), titania nanorods (TNRs) and titania nanochain (TNCs)

Formation procedures of single crystal-like network structure of TNWs and TNRs have been reported in our previous reports [36,37]. Formation procedure of TNCs is almost the same as that of formation procedure of TNRs, except usage of HCl instead of ethylenediamine to adjust pH values to 1.3–5.

2.2. Preparation of titania thin films and solar cells

We have synthesized titania nanoparticles (TNPs) with diameter of 3–5 nm [38,39] in addition to 1DTNM described above. The TNPs and P-25 were used for stabilizing structurally the 1DTNM electrode films. Fluorine doped tin oxide (FTO) was used as an electric conducting oxide. In the case of TNWs, a gel solution of TNWs mixed with P-25 was made by mixing the gel solution of P-25 with reaction products of TNWs in a gel state after centrifugation. Here, the aqueous gel solution of P-25 with polyethylene glycol (PEG) was made after the procedure reported by Grätzel's group [4]. Solar cells were fabricated as follows. First, the gel solution of TNPs with 3–5 nm in diameter was coated 3 times by doctor blade on FTO. The gel solution of TNWs mixed with P-25 was coated by doctor blade method by 8–10 times. In the case of cells made of TNRs, the reaction product after centrifugation was mixed with gel solutions of TNPs. The mixed gel solution was coated by 7–10 times on FTO. In the case of TNCs, the procedure was the same as the case of TNRs.

After each coating, the sample was calcined at 773 K for 10 min. The last calcination was made for 30 min at 773 K. And then dye was introduced to the titania thin films by soaking the film 1–3 days in 3×10^{-4} M solution of a ruthenium dye in a mixed solvent of tert-butanol and acetonitrile. Cis-di(thiocyanate) bis(2,2′-bipyridyl-4,4′-di-carboxylate)-ruthenium(II) bis-tetra-butyl-ammonium (N719) (Solaronix SA) produced by Grätzel's group [4] was used as the dye.

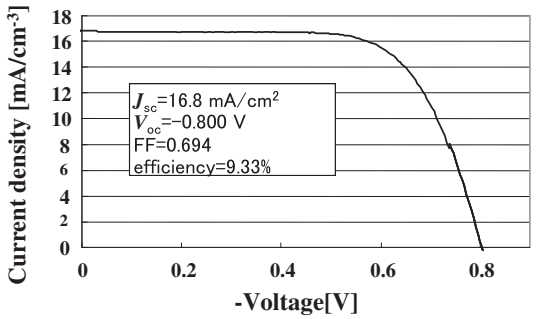

Fig. 2. *I–V* curve obtained for a cell with a complex electrode composed of network structure of single crystal-like titania nanowires, titania nanoparticles and P-25.

The DSSCs were comprised of a titania thin film electrode on a conducting glass plate, and a platinum electrode made by sputtering on the conducting glass and an electrolyte layer between the titania thin film and the platinum. The composition of the used electrolyte was 0.1 M guanidinium thiocyanate, 0.6 M 1-butyl-3-methylimidazolium iodide, 0.03 M I_2, and 0.5 M TBP (4-tert-butylpyridine) in the mixed solvent of acetonitrile and n-valeronitrile (volume 85:15). The cell size was 0.25 cm^2.

2.3. Characterization

Characterization of the produced materials was performed by X-ray diffraction (XRD) (Rigaku Goniometer PMG-A2, CN2155D2), transmission electron microscopy (TEM) and selected-area electron diffraction (SAED) (JEOL 200 CX and JEM-2100F), scanning electron microscopy (SEM) (JEOL JSM 7500FA) and isotherm of nitrogen adsorption (BEL SORP 18 PLUS). The photo-current–voltage characteristics were measured using an AM 1.5 solar simulator (YSS-E40, Yamashita Denso), in which the light intensity is 100 mW cm^{-2} calibrated with a secondary reference solar cell standardized by JET (Japan Electrical Safety & Environmental Technology Laboratories). Electron transport processes were measured by electrochemical impedance spectroscopy (EIS) (Solartron 1255B).

3. Results and discussion

3.1. Highly efficient dye-sensitized solar cells obtained by utilization of one-dimensional titania nanoscale materials

We succeeded in synthesis of TNWs [36], TNRs [37] and recently TNCs (see Fig. 1). We applied these materials for DSSCs, and present

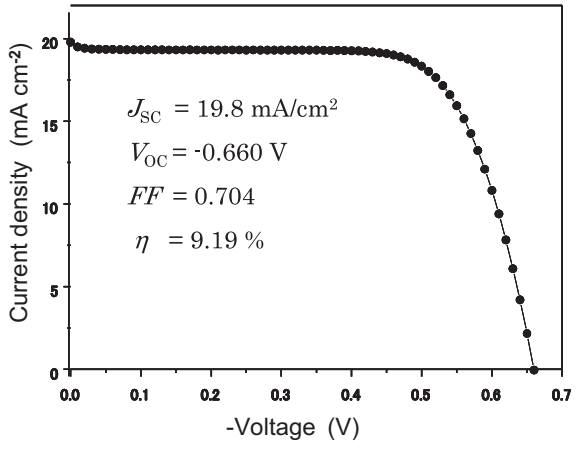

Fig. 3. *I–V* curve obtained for the cell composed of one-dimensional TNCs mixed with TNPs [38,39].

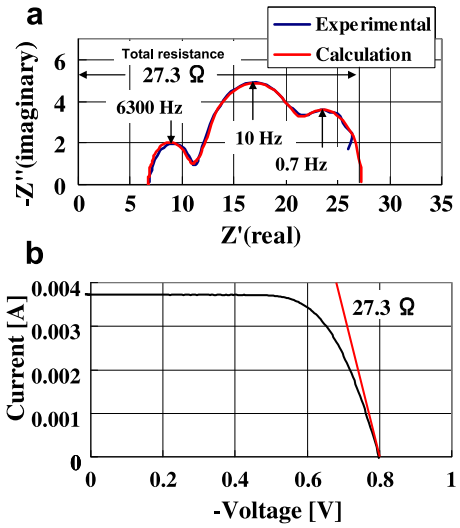

Fig. 4. (a) Typical Nyquist plot obtained by EIS, (b) *I–V* curve for the same cell.

here that highly crystalline 1DTNM are effective to attain high light-to-electricity conversion yield. As shown in our previous paper [36], network structure of single crystal-like TNWs can be synthesized successfully by the oriented attachment mechanism. We attained 9.33% conversion efficiency with complex titania electrode made of TNWs and P-25. Recently, we attained the same conversion efficiency 9.33% using different electrolyte from the previous (Fig. 2). In our previous paper [36], we used an electrolyte composed of 0.1 M of LiI, 0.6 M of 1,2-dimethyl-3-n-propylimidazolium iodide, 0.05 M of I_2, 1 M of 4-tert-butylpyridine in methoxyacetonitrile and got 9.33% conversion efficiency with short circuit current density $J_{sc} = 19.2$ mA cm^{-2}, open circuit voltage $V_{oc} = 0.72$ V and fill factor 0.675. In the present result, by using the new electrolyte described in the experimental Section 2.2, V_{oc} value of 0.8 V is larger than that of previous one 0.72 V, because guanidinium thiocyanate decreased redox potential of I^-/I_3^- in the present electrolyte. Unfortunately, we got a lower short circuit current density $J_{sc} = 16.8$ mA cm^{-2} than that of our previous one, and the same efficiency was obtained.

Highly crystallized TNRs have been synthesized by hydrothermal process using blockcopolymer (F127) and surfactant cetyltrimethylammonium bromide (CTAB) as a mixed template [37]. TNRs with 100–300 nm in length and 20–30 nm in diameter was obtained. A high-resolution TEM (HRTEM) image of single TNR shows that titanium atoms align perfectly in titania anatase crystalline structure with no lattice defect, and the surface of TNR is

Table 1
Performance of dye-sensitized solar cells with various TNW content.

Content	J_{sc} [mA cm^{-2}]	V_{oc} [V]	FF	η [%]	Thickness [μm]
0 wt%	10.93	0.85	0.74	6.85	10
0 wt%	11.82	0.82	0.71	6.87	26
0 wt%	10.92	0.80	0.71	6.20	35
5 wt%	11.98	0.85	0.73	7.48	19
5 wt%	10.96	0.81	0.73	6.50	32
10 wt%	12.84	0.84	0.73	7.87	18
10 wt%	12.68	0.84	0.72	7.64	20
28 wt%	14.88	0.82	0.71	8.66	24
28 wt%	13.09	0.83	0.74	8.04	27
50 wt%	13.39	0.85	0.71	8.02	14
50 wt%	15.18	0.80	0.70	8.51	22
100 wt%	11.94	0.84	0.73	7.28	5
100 wt%	9.93	0.82	0.71	5.75	9
100 wt%	10.16	0.84	0.70	5.97	11

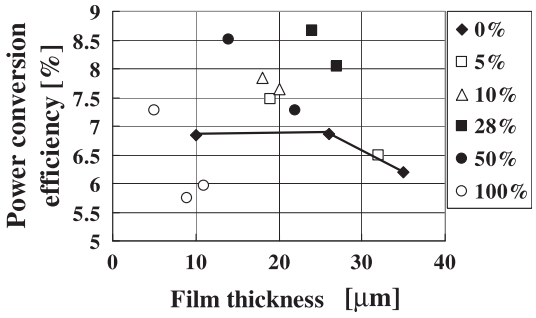

Fig. 5. Effect of content of TNWs on power conversion efficiency.

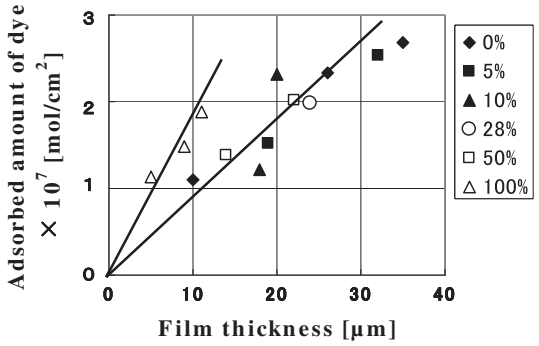

Fig. 7. Relationship between film thickness and the adsorbed amount of dye.

facetted with the TiO_2 anatase {101} faces [40]. The observed fringes are {101} planes of anatase TiO_2 with a lattice spacing of about 0.351 nm, which agrees with the value recorded in JCPDS card. The highly crystallized TNRs were used to fabricate a titania electrode of DSSCs. The complex electrodes were made by the repetitive coating-calcining process: 3 layers of TNPs were first coated on FTO conducting glass, followed by 8 layers of mixed gel composed of TNRs and TNPs. A high light-to-electricity conversion efficiency of 8.93% was achieved [40].

We have newly synthesized TNCs as shown in Fig. 1. The formation procedure was the same as that of TNRs (see Ref. [37]), except no use of ethylenediamine and adjusting pH of the aqueous solution of tetra-isopropylorthotitanate (TIPT), F127 and CTAB to acidic conditions by adding hydrochloric acid; pH = 1.3–5.0. Highly crystallized titania nanoparticles with diameter of around 10 nm combine with each other and make chains. The obtained white solid product was mixed with spherical TNPs (3–5 nm in diameter) [38,39] to fabricate titania film electrodes for DSSCs. The I–V curve of the cell is shown in Fig. 3. The obtained light-to-electricity conversion yield of the cell was 9.2%.

All three kinds of one-dimensional titania nanoscale materials mentioned above show high light-to-electricity conversion yield around 9%, suggesting strongly that highly crystallized one-dimensional titania materials are essentially important for attainment of high efficient dye-sensitized solar cells.

3.2. Theoretical consideration on necessity of highly crystallized titania nanoscale materials

First, let us consider the reason why highly crystallized one-dimensional titania materials are needed. Fig. 4(a) shows a typical Nyquist plot obtained by EIS under open circuit condition. Total direct current (dc) resistance at V_{oc} is given by the length from 0 to the point at $\omega = 0$ on the real axis as shown by Fig. 4(a). This fact is confirmed by reproduction of I–V curve using measured total dc resistances at various bias voltages as shown in Fig. S1 (Supplementary data). Total dc resistance is also obtained from the slope of the tangent line at the point of V_{oc} (Fig. 4(b)). When the total dc resistance becomes small, the slope becomes steep, and the fill factor becomes larger, resulting in a higher light-to-electricity conversion efficiency. Thus, the total dc resistance should be small. However, the largest arc of around 10 Hz in Fig. 4(a) represents the resistance of recombination reactions between electrons in the titania electrode and I_3^- ions in the electrolyte, R_k. Small total dc resistance means small resistance for recombination reactions, indicating rapid reaction rate of recombination. Thus, such small total dc resistance seems an obstacle for attainment of highly efficient solar cells. But, whether electrons in the titania electrode are properly collected by the transparent conducting glass electrode or react with I_3^- ions in the electrolyte by recombination reactions is determined in actual fact by the ratio of the resistance for the transport rate to the conducting glass electrode (R_w) against the resistance for the recombination reactions (R_k). When R_w is much smaller than R_k, almost all electrons are properly collected by the conducting glass electrode. This means that the transport rate of electrons in the titania electrode should be very rapid, indicating that we need nice titania materials with high electron transport rate, i.e., highly crystallized one-dimensional nanoscale TiO_2 materials are needed.

Many researchers familiar with EIS measurement know that highly efficient dye-sensitized solar cells show small total resistance of the cell, i.e., narrow Nyquist spectrum. They also know that largest arc of Nyquist plot represents the resistance for recombination reactions R_k. This apparent conflict can be solved clearly by theoretical consideration through recognition that the large value of the ratio R_k/R_w is essentially important for the highly efficient cells, and the absolute value of R_k is not important, i.e., very small R_w is indispensable for the highly efficient cells.

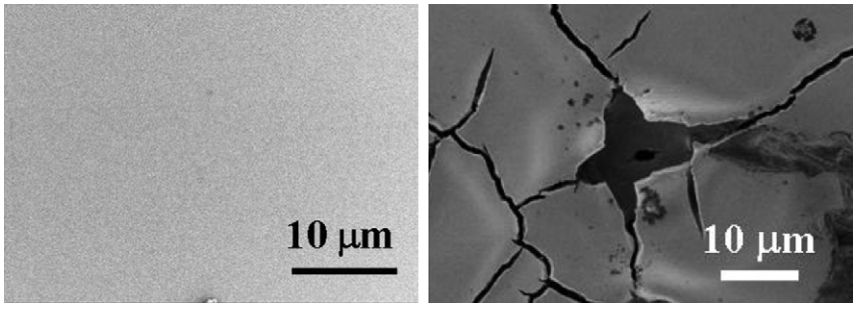

Fig. 6. Top views of 100% TNW films. Film thickness; left: 5 μm, right: 11 μm.

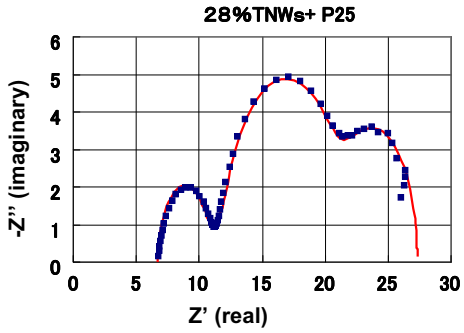

Fig. 8. Nyquist plot of the cell with electrode of 28% TNWs with P-25 as one example.

3.3. *Verification of the theoretical consideration by experiments*

In order to verify the theoretical consideration by experiments, dye-sensitized solar cells with electrodes made of TNWs and P-25 with various TNW content were made. TNWs were chosen as a 1DTNM. The TNW content was changed from 0% to 100%. The content of TNW was defined as percentage of titanium atoms of TNWs in the total titanium atoms included in the titania electrode. Table 1 shows performance of DSSCs with various TNW content, i.e., the current density J_{sc}, open circuit voltage V_{oc}, fill factor FF and power conversion efficiency η, together with film thickness. Effect of TNW content on power conversion efficiency (PCE) is summarized in Fig. 5. PCE of the cells including TNWs are higher than those cells without TNWs (denoted with lines in the figure), indicating that TNWs is useful to attain high efficiency except 100% TNW case. When the film thickness of 100% TNW cells increased larger than 9 μm, peel off of the films with cracks was observed by SEM images as shown in Fig. 6, resulting that less than 6% of PCE were observed as shown in Table 1 and Fig. 5. Thus, mixing of TNWs with P-25 nanoparticles is important to make robust films.

Since the amount of adsorbed dyes is another important factor to affect PCE, the amounts of adsorbed dyes for the cells with various TNW contents are shown as a function of film thickness in Fig. 7. The amount of adsorbed dye in the cells containing TNWs from 0% to 50% locates nearly in the same straight line regardless of the difference in TNW contents, except 100% TNW which shows higher adsorbed amounts. This higher adsorption of 100% TNW is attributable to the smaller diameter of TNW of 3–7 nm, which is much smaller than the diameter of 23 nm of P-25. Thus the measured specific surface area of 100% TNWs 78 m^2/g is much higher than that of P-25 45 $m^2\ g^{-1}$. The specific surface area was measured after calcinations at 773 K for 30 min. We have interesting data of specific surface area of 28% TNWs with P-25; 48 $m^2\ g^{-1}$. This value is closer to the pure P-25 and is much smaller than that of the 100% TNWs. This difference in specific surface area between the 28% TNW with P-25 and the pure 100% TNWs corresponds well to the difference in adsorbed dye amount between the TNWs with P-25 at 0–50% and the pure 100% TNWs. These findings suggest some interesting structural change in the surface of the mixture of TNW and P-25. However, the reason why the cells containing different TNW content from 0% to 50% locates in the same straight line in Fig. 7 is not well understood at present.

EIS measurements for the cells containing various TNW contents shown in Table 1 were carried out. Fig. 8 shows Nyquist plot of a cell with electrode of 28% TNWs with P-25 as an example.

Table 2
Parameters determined by EIS analysis for the cells with various TNW content.

TNW [%]	0	0	0	5	5	5	10	10	10	10
Con=	0.309	0.397	0.4	0.316	0.257	0.33	0.22	0.224	0.277	0.23
D_{eff}=	0.000038	0.000093	0.00024	0.0000747	0.000095	0.00025	0.00009	0.000085	0.00022	0.00015
L=	0.001	0.00264	0.0035	0.00191	0.00191	0.0032	0.0018	0.0018	0.002	0.002
k_{eff}=	13.8	7.67	13.8	7.67	7.67	13.8	7.67	7.67	16.3	13.8
$R_{I_3^-}$ =	7.7	7	7	8	7.6	6.5	9.1	8.1	5.1	6.4
$D_{I_3^-}$ =	0.00001	0.000004	0.00000295	0.000007	0.0000068	0.00000328	0.0000027	0.0000057	0.0000045	0.0000045
δ=	0.005	0.005	0.005	0.005	0.005	0.005	0.005	0.005	0.005	0.005
R_{Pt}=	3.5	6.7	4.8	15	5.8	3.5	4.25	3.4	7	4.6
C_{Pt}=	0.00006	0.000046	0.000055	0.0000313	0.0000675	0.00005	0.00005	0.00006	0.00004	0.000065
R_{sub}=	7.96	8.9	9.8	12	11.79	10.4	8.69	8.92	8.5	9.8
R_k/R_w=	2.75	1.74	1.42	2.67	3.4	1.77	3.62	3.42	3.37	2.72
R_w=	8.13	11.3	5.83	8.08	5.17	4.22	4.4	4.74	2.52	3.07
R_k=	22.4	19.6	8.28	21.6	17.5	7.47	15.9	16.2	8.5	8.33
n=	2.17×10^{18}	1.69×10^{18}	1.67×10^{18}	2.11×10^{18}	2.6×10^{18}	2.03×10^{18}	3.04×10^{18}	2.99×10^{18}	2.42×10^{18}	2.91×10^{18}

TNW [%]	28	28*	50	50	50	50	100	100	100
Con=	0.165	0.225	0.206	0.217	0.251	0.15	0.161	0.154	0.185
D_{eff}=	0.0001	0.00012	0.00014	0.00018	0.00015	0.000104	0.000072	0.000023	0.00015
L=	0.002	0.002	0.00139	0.00139	0.0022	0.0022	0.000925	0.000505	0.0009
k_{eff}=	10	12.5	18.65	19.9	7.67	5	8	10.32	18
$R_{I_3^-}$ =	5.6	5.8	6.9	6.9	9.5	11.5	14.5	13.4	11
$D_{I_3^-}$ =	0.000007	0.0000055	0.000005	0.0000053	0.000003	0.0000035	0.000011	0.0000096	0.00000352
δ=	0.005	0.005	0.005	0.005	0.005	0.005	0.005	0.005	0.005
R_{Pt}=	2	2.8	3	9.85	5	3.88	4	5.8	5.7
C_{Pt}=	0.0001	0.00006	0.000038	0.00006	0.0000577	0.000045	0.000052	0.00005	0.0000433
R_{sub}=	5.6	5.8	9.12	10.1	8.21	8.07	8	10.7	11
R_k/R_w=	2.5	2.4	3.89	4.68	4.04	4.3	10.5	8.74	10.3
R_w=	3.3	3.75	2.04	1.68	3.68	3.17	2.07	3.38	1.11
R_k=	8.25	9	7.94	7.84	14.9	13.6	21.8	29.5	11.4
n=	3.89×10^{18}	2.85×10^{18}	3.25×10^{18}	3.08×10^{18}	2.67×10^{18}	4.46×10^{18}	4.16×10^{18}	4.35×10^{18}	3.62×10^{18}

Con $= k_BT/q^2An$ [Ω cm s^{-1}], where k_B [J K^{-1}] represents Boltzmann constant, T [K] is absolute temperature, q [C] is elementary charge, A [cm^2] is area of the cell and n [cm^{-3}] is electron density.
Con: constant inversely proportional to the electron density, D_{eff} [$cm^2\ s^{-1}$]: diffusion coefficient of electron, L [cm]: film thickness of TiO_2 electrode, k_{eff} [s^{-1}]: reaction rate constant of recombination reactions, $R_{I_3^-}$ [Ω]: diffusion resistance of I_3^-, $D_{I_3^-}$ [$cm^2\ s^{-1}$]: diffusion coefficient of I_3^-, δ [cm]: thickness of the electrolyte phase, R_{Pt} [Ω]: resistance of Pt electrode, C_{Pt} [F]: capacity of Pt electrode, R_{sub} [Ω]: resistance of substrate, R_w [Ω]: resistance for electron transport in the TiO_2 electrode, R_k [Ω]: resistance for recombination reaction.

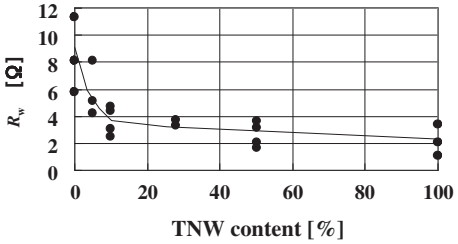

Fig. 9. Relationship between R_w and TNW content.

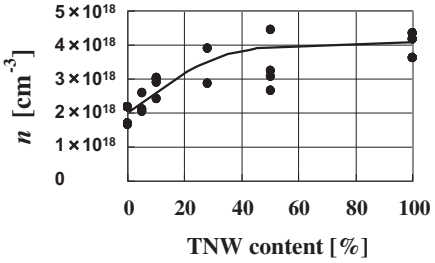

Fig. 11. Relationship between electron density n and TNW content.

The plotted squares in Fig. 8 represent experimental results, and the solid curve shows the calculated spectrum from the following equations (1)–(4) using parameters shown in Table 2 for 28% TNWs (indicated by 28* in the table) [41].

Impedance equations for electron transport processes are given as follows [41], where ω is frequency, ω_k and ω_d are defined by equation (2) and R_w, D_{eff}, L, k_{eff}, k_B, T, q, A, n, Con, R_k R_{Pt}, C_{Pt}, $R_{I_3^-}$, $D_{I_3^-}$, and δ are shown in the footnote of Table 2. For the impedance, Z, concerning with titania electrode, equation (1) was derived:

$$Z = R_w \left(\frac{1}{\left(\frac{\omega_k}{\omega_d}\right)\left(1+\frac{i\omega}{\omega_k}\right)} \right)^{1/2} \coth\left[\left(\frac{\omega_k}{\omega_d}\right)\left(1+\frac{i\omega}{\omega_k}\right) \right]^{1/2} \quad (1)$$

$$\text{here,} \quad \omega_d = \frac{D_{eff}}{L^2}, \quad \omega_k = k_{eff}, \quad R_w = \frac{k_B T}{q^2 A n}\frac{L}{D_{eff}} = \text{Con}\frac{L}{D_{eff}}, \quad R_k = \text{Con}\frac{1}{L k_{eff}} \quad (2)$$

For the impedance, Z_{Pt}, concerning with platinum electrode, equation (3) was assumed:

$$Z_{Pt} = \frac{R_{Pt}}{1 + i\omega R_{Pt} C_{Pt}} \quad (3)$$

For the impedance, Z_N, concerning with tri-iodide diffusion, the finite Warburg impedance equation, i.e., equation (4) was assumed:

$$Z_N = R_{I_3^-} \frac{1}{\sqrt{\frac{i\omega}{\left(D_{I_3^-}/\delta^2\right)}}} \tanh \sqrt{\frac{i\omega}{\left(D_{I_3^-}/\delta^2\right)}} \quad (4)$$

The calculated solid curves in Fig. 8 agree quite well with the plotted experimental data. The characteristics of electron transport properties of the cells with electrodes made of TNWs and P-25 were examined by the determined parameters shown in Table 2. Resistance for electron transport from a titania electrode to a transparent conducting glass electrode R_w are plotted against TNW content in Fig. 9. R_w values decrease steeply up to 10% of TNW content and become gradual decrease after 20% of TNW content. This decrease indicates clearly that electron transport in the titania electrode is improved by mixing TNWs with P-25 nanoparticles. The ratios of R_k representing the resistance for the recombination reactions to R_w are plotted against TNW content in Fig. 10. The ratio of R_k/R_w increases with increase in TNW content. This shows that TNWs restrains the recombination reactions between electrons in the titania electrode and I_3^- ions in the electrolyte and contributes to collect electrons properly to the transparent conducting glass electrode. The findings shown in Figs. 9 and 10 bring the high electron density in the titania electrode as shown in Fig. 11.

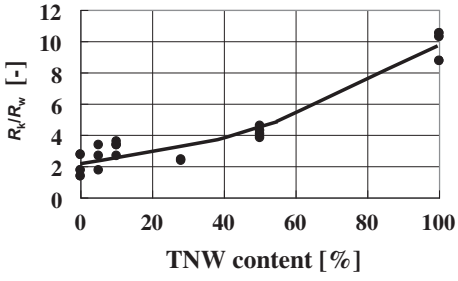

Fig. 10. Relationship between R_k/R_w and TNW content.

The above results and discussion are summarized as below. The experimental results of I–V and EIS measurements of TNWs with P-25 with various TNW content clearly showed the following three points as characteristics of highly crystalline 1-dimensional titania nanoscale material TNWs. 1) Resistance of electron transport in the titania electrode R_w is small. 2) The ratio of resistance R_k/R_w is large, i.e., efficiency of electron collection is high. 3) Electron density n in the titania electrode is high.

4. Conclusions

1. All cells composed of three kinds of highly crystallized 1DTNM, i.e., network structure of titania nanowires, titania nanorods, and titania nanochains, show high power conversion efficiency about 9%.
2. Necessity of highly crystallized 1DTNM is elucidated by theoretical consideration based on both the electron transfer processes shown by Nyquist plot obtained by EIS and I–V measurements.
3. The measurements of I–V relationship and EIS of the cells with electrodes made of various TNW content with P-25 show clearly following three points as verification of the consideration; 1) resistance of electron transport in the titania electrode to the conducting glass electrode is small, 2) the ratio of the resistance for the recombination reactions against the resistance for the transport rate to the conducting glass electrode is large, i.e., efficiency of electron collection is high, and 3) electron density in the titania electrode is high.

Appendix A. Supplementary data

Supplementary data of reproduction of I–V curve by the total resistance determined by EIS can be found, in the online version, at http://dx.doi.org/10.1016/j.jpowsour.2012.10.024.

References

[1] V.S. Arunachalam, E.L. Fleischer, MRS Bull. 33 (2008) 264–276.

[2] A.S. Nair, Z. Peining, V.J. Babu, Y. Shengyuan, S. Ramakrishna, Phys. Chem. Chem. Phys. 13 (2011) 21248–21261.
[3] B. O'Regan, M. Grätzel, Nature (London) 353 (1991) 737–740.
[4] M.K. Nazeeruddin, A. Kay, I. Rodicio, B.R. Humphry, E. Mueller, P. Liska, N. Vlachopoulous, M. Grätzel, J. Am. Chem. Soc. 115 (1993) 6382–6390.
[5] A. Yella, H.-W. Lee, H.N. Tsao, C. Yi, A.K. Chandiran, M.K. Nazeeruddin, E.W.-G. Diau, C.-Y. Yeh, S.M. Zakeeruddin, M. Grätzel, Science 334 (2011) 629–634.
[6] S. Ito, P. Liska, P. Comt, R.L. Charvet, U. Back, L. Schmidt-Mende, S.M. Zakeeruddin, A. Kay, M.K. Nazeeruddin, M. Grätzel, Chem. Commun. (2005) 4351–4353.
[7] Z.P. Zhang, S. Ito, B. O'Regan, D.B. Kuang, S.M. Zakeeruddin, P. Liska, R. Charvet, M.K. Nazeeruddin, P. Pechy, R. Hunphry-Baker, T. Koyanagi, T. Mizuno, M. Grätzel, Z. Phys. Chem. 221 (2007) 319–328.
[8] Z.-S. Wang, H. Kawauchi, T. Kashima, H. Arakawa, Coord. Chem. Rev. 248 (2004) 1381–1389.
[9] S. Hore, P. Nitz, C. Vetter, C. Prahl, M. Niggemann, R. Kern, Chem. Commun. (2005) 2011–2013.
[10] C. Barbe, F. Arendse, P. Comte, M. Jirousek, F. Lenzmann, V. Shklover, M. Grätzel, J. Am. Ceram. Soc. 80 (1997) 3157–3171.
[11] B.C. O'Regan, J.R. Durrant, P.M. Sommeling, N.J. Bakker, J. Phys. Chem. C 111 (2007) 14001–14010.
[12] P.M. Sommeling, B.C. O'Regan, R.R. Hsawell, H.J.P. Smit, N.J. Bakker, J.J.T. Smit, J.M. Kroon, J.A.M. van Roosmalen, J. Phys. Chem. B 110 (2006) 19191–19197.
[13] H. Lindström, A. Holmberg, E. Magnusson, S.-E. Lindquist, L. Malmqvist, A. Hagfeldt, Nano Lett. 1 (2001) 97–100.
[14] T. Yamaguchi, N.T. Matsumoto, H. Arakawa, Chem. Commun. (2007) 4767–4769.
[15] M. Adachi, Y. Murata, I. Okada, S. Yoshilkawa, J. Electrochem. Soc. 150 (2003) G488–G493.
[16] Y. Ohsaki, T. Masaki, Y. Kitamura, Y. Wada, T. Okamoto, T. Sekino, K. Niihara, S. Yanagida, Phys. Chem. Chem. Phys. 7 (2005) 4157–4163.
[17] T. Kasuga, M. Hiramatsu, A. Hosono, T. Sekino, K. Niihara, Langmuir 14 (1998) 3160–3163.
[18] T. Kasuga, M. Hiramatsu, A. Hosono, T. Sekino, K. Niihara, Adv. Mater. 11 (1999) 1307–1311.
[19] P.-T. Hsiao, K.-P. Wang, C.-W. Cheng, H. Teng, J. Photochem. Photobiol. A 188 (2007) 19–24.
[20] G.-S. Kim, H.-K. Seo, V.P. Godble, Y.-S. Kim, O.-B. Yang, H.-S. Shin, Electrochem. Commun. 8 (2006) 961–966.
[21] M. Wei, Y. Konishi, H. Zhou, H. Sugihara, H. Arakawa, J. Electrochem. Soc. 153 (2006) A1232–A1236.
[22] K. Zhu, R. Neale, A. Miedaner, A.J. Frank, Nano Lett. 7 (2007) 69–74.
[23] D. Kuang, J. Brillet, P. Chen, M. Takata, S. Uchida, K. Miura, K. Sumioka, S.M. Zakeeruddin, M. Grätzel, ACS Nano 2 (2008) 1113–1116.
[24] Z. Liu, M. Misra, ACS Nano 4 (2010) 2196–2200.
[25] M. Ye, X. Xin, C. Lin, Z. Lin, Nano Lett. 11 (2011) 3214–3220.
[26] H. Jha, P. Roy, R. Hahn, I. Paramasivam, P. Schmuki, Electrochem. Commun. 13 (2011) 302–305.
[27] B.-X. Lei, J.-Y. Liao, R. Zhang, J. Wang, C.-Y. Su, D.-B. Kuang, J. Phys. Chem. C 114 (2010) 15228–15233.
[28] C.-J. Lin, W.-Y. Yu, S.-H. Chein, J. Mater. Chem. 20 (2010) 1073–1077.
[29] J. Liu, Y.-T. Kuo, K.J. Klabunde, C. Rochford, J. Wu, J. Li, ACS Appl. Mater. Interface 1 (2009) 1645–1649.
[30] S. Muduli, W. Lee, V. Dhas, S. Mujawar, M. Dubey, K. Vijayamohanan, S.-H. Han, S. Ogale, ACS Appl. Mater. Interface 1 (2009) 2030–2035.
[31] T.-Y. Lee, P.S. Alegaonkar, J.-B. Yoo, Thin Solid Films 515 (2007) 5131–5135.
[32] X. Dang, H. Yi, M.-H. Ham, J. Qi, D.S. Yun, R. Ladewski, M.-S. Strano, P.-T. Hammond, A.M. Belcher, Nat. Nanotechnol. 6 (2011) 377–384.
[33] M.-Y. Song, D.-K. Kim, K.-J. Ihn, S.M. Jo, D.Y. Kim, Nanotechnology 15 (2004) 1861–1865.
[34] B.-H. Lee, M.Y. Song, S.-Y. Jang, S.-M. Jo, S.-Y. Kwak, D.-Y. Kim, J. Phys. Chem. C 113 (2009) 21453–21457.
[35] A.S. Nair, Y. Shengyuan, Z. Peining, S. Ramakrishna, Chem. Commun. 46 (2010) 7421–7423.
[36] M. Adachi, Y. Murata, J. Takao, J. Jiu, M. Sakamoto, F. Wang, J. Am. Chem. Soc. 126 (2004) 14943–14949.
[37] J. Jiu, S. Isoda, F. Wang, M. Adachi, J. Phys. Chem. B 110 (2006) 2087–2092.
[38] J. Jiu, F. Wang, M. Sakamoto, J. Takao, M. Adachi, J. Electrochem. Soc. 151 (2004) A1653.
[39] J. Jiu, S. Isoda, M. Adachi, F. Wang, J. Photochem. Photobiol. A Chem. 189 (2007) 314–321.
[40] K. Yoshida, J. Jiu, D. Nagamatsu, T. Nemoto, H. Kurata, M. Adachi, S. Isoda, Mol. Crystals Liquid Crystals 491 (2008) 14–20.
[41] M. Adachi, M. Sakamoto, J. Jiu, Y. Ogata, S. Isoda, J. Phys. Chem. B 110 (2006) 13872–13880.